

Predication of novel effects in rotational nuclei at high speed

Jian-You Guo^{1,*}

¹*School of physics and Optoelectronic Engineering, Anhui University, Hefei 230601, China*

(Dated: September 6, 2023)

The study of high-speed rotating matter is a crucial research topic in physics due to the emergence of novel phenomena. In this paper, we combined cranking covariant density functional theory (CDFT) with a similar renormalization group approach to decompose the Hamiltonian from the cranking CDFT into different Hermit components, including the non-relativistic term, the dynamical term, the spin-orbit coupling, and the Darwin term. Especially, we obtained the rotational term, the term relating to Zeeman effect-like, and the spin-rotation coupling due to consideration of rotation and spatial component of vector potential. By exploring these operators, we aim to identify novel phenomena that may occur in rotating nuclei. Signature splitting, Zeeman effect-like, spin-rotation coupling, and spin current are among the potential novelties that may arise in rotating nuclei. Additionally, we investigated the observability of these phenomena and their dependence on various factors such as nuclear deformation, rotational angular velocity, and strength of magnetic field.

I. INTRODUCTION

The investigation of the structure and property of matter under extreme conditions is an important research subject for physicists. With the development of accelerator facilities, particle detector systems, and techniques of nuclear spectroscopy, physicists have discovered many novel phenomena with unexpected features in atomic nuclei. These novel phenomena include neutron (proton) halos [1, 2], energy level inversion [3, 4], change of magic numbers [5–7], exotic radioactivity [8, 9], high spin states [10, 11], and others

The high-spin states provide an important opportunity to investigate the microscopic mechanism of deformed shell structure, single-particle motion, and collective excitation. Since the discovery of backbending phenomenon in high spin states [12], the rotation excitation has become an active frontier. The backbending [12, 13], band termination [14, 15], signature inversion [16], superdeformed rotation [10, 11], magnetic and antimagnetic rotations [17, 18], chiral rotation [19] have attracted worldwide attention.

To understand these novel phenomena associated with rotational excitation, physicists have developed various theoretical models, such as the cranked Nilsson-Strutinsky method [20], the cranked shell model [21], the projected shell model [22], the tilted-axis cranking model [18], large-scale shell model calculations [23], and density functional theories [24, 25]. However, these models have limitations due to the breaking of time-reversal symmetry by the Coriolis operator and unpaired nucleons, which results in time-odd components that are difficult to treat in non-relativistic framework.

The self-consistent cranking covariant density functional theory (CDFT) has successfully described the rotational excitations of atomic nuclei [26, 27], including the

magnetic rotation, antimagnetic rotation, chiral doublet bands [19, 28], and multiple chiral doublets [29–32], and it can handle time-odd fields corresponding to nonzero spatial component of the vector potential, which is important for understanding these novel phenomena. Additionally, the CDFT with point-coupling interactions was developed [33] and applied successfully to magnetic and antimagnetic rotations [34].

Although the cranking CDFT provides an excellent description of rotational excitations, the novel effects hidden in the cranking Dirac Hamiltonian have not been fully revealed. In Refs. [35, 36], we have applied the similarity renormalization group (SRG) to decompose the Dirac Hamiltonian from the relativistic mean field into different components, and obtained the non-relativistic term, dynamical term, spin-orbital coupling, and Darwin term. Based on these operators, we have clarified the origin and breaking mechanism of spin and pseudospin symmetries in spherical nuclei [37–39] as well as deformed nuclei [40]. Following our scheme, an analytic expansion to the $1/M^4$ order is obtained in Ref. [41] in comparison with the improvement by replacing M with $M + S(r)$. A similar work has been done in Ref. [42].

In this study, we have combined the cranking CDFT with SRG to disclose the novel phenomena that may arise in rotating nuclei. By decomposing the Hamiltonian from the cranking CDFT, we have obtained three additional operators: the rotational term, the term relating to Zeeman effect, and the spin-rotation coupling due to consideration of rotation and spatial component of vector potential. Based on these operators, we explore the novel phenomena that may occur in high-speed rotating nuclei, which is interesting and expects to be observed in experiment. Especially, the spin rotation coupling is the cause of spin current generation. The spin current, which is a key concept in the field of spintronics [43], and can be employed to probe intriguing properties of quantum materials [44], and understand the spin Hall effect [45]. It is worth looking forward to whether this phenomenon occurs in high-speed rotating nuclei or high-speed rotating neutron stars.

*Corresponding author: jianyou@ahu.edu.cn

The theoretical formalism is presented in section II. The numerical details and results are presented in section III. A summary is given in section IV.

II. DECOMPOSITION OF CRANKING DIRAC HAMILTONIAN WITH SIMILARITY RENORMALIZATION GROUP

To investigate the potential emergence of novel phenomena in high-speed rotating nuclei or neutron stars, we have applied the SRG method to decompose the Dirac Hamiltonian from the cranking CDFT. Within the cranking CDFT, the Dirac equation describing rotating nuclei is represented as:

$$H\psi = \varepsilon\psi, \quad (1)$$

with the Dirac Hamiltonian

$$H = \vec{\alpha} \cdot \vec{\pi} + \beta(M + S) + V - \vec{\Omega} \cdot \vec{J}, \quad (2)$$

where $\vec{\pi} = \vec{p} - \vec{V}$ and $\vec{J} = \vec{r} \times \vec{\pi} + \vec{\Sigma}$ with $\vec{\Sigma} = \frac{\hbar}{4i} \vec{\alpha} \times \vec{\alpha}$. The scalar potential $S(\vec{r})$ and vector potential $V_\mu(\vec{r})$ from the CDFT are represented in the following form:

$$\begin{aligned} S(\vec{r}) &= g_\sigma \sigma(\vec{r}), \\ V(\vec{r}) &= g_\omega \omega_0(\vec{r}) + g_\rho \tau_3 \rho_{30}(\vec{r}) + e \frac{1 - \tau_3}{2} A_0(\vec{r}), \\ \vec{V}(\vec{r}) &= g_\omega \vec{\omega}(\vec{r}) + g_\rho \tau_3 \vec{\rho}_3(\vec{r}) + e \frac{1 - \tau_3}{2} \vec{A}(\vec{r}). \end{aligned} \quad (3)$$

To reveal the underlying physics hidden in the cranking Dirac Hamiltonian, we transform it into a Schrödinger-like form using SRG. The initial Hamiltonian H is transformed by the unitary operator $U(l)$ according to

$$H(l) = U(l) H U^\dagger(l), \quad H(0) = H \quad (4)$$

where l is a flow parameter. Differentiation of Eq.(4) gives the flow equation as

$$\frac{d}{dl} H(l) = [\eta(l), H(l)], \quad (5)$$

with the generator $\eta(l) = \frac{dU(l)}{dl} U^\dagger(l)$. The choice of $\eta(l)$ is to make $H(l)$ diagonal in the limit $l \rightarrow \infty$. For the present Hamiltonian, it is appropriate to choose $\eta(l)$ in the form

$$\eta(l) = [\beta M, H(l)]. \quad (6)$$

In order to solve Eq.(5), the Hamiltonian $H(l)$ is presented as a sum of even operator $\varepsilon(l)$ and odd operator $o(l)$:

$$H(l) = \varepsilon(l) + o(l), \quad (7)$$

where the even or oddness is defined by the commutation relations of the respective operators, i.e., $\varepsilon(l)\beta = \beta\varepsilon(l)$ and $o(l)\beta = -\beta o(l)$. The system can be solved

perturbatively by the expansions of $\varepsilon(\lambda)$ and $o(\lambda)$ as follows

$$\begin{aligned} \frac{1}{M} \varepsilon(\lambda) &= \sum_{i=0}^{\infty} \frac{1}{M^i} \varepsilon_i(\lambda), \\ \frac{1}{M} o(\lambda) &= \sum_{j=1}^{\infty} \frac{1}{M^j} o_j(\lambda). \end{aligned} \quad (8)$$

As $\varepsilon(0) = \beta(M + S) + V - \vec{\Omega} \cdot \vec{J}$ and $o(0) = \vec{\alpha} \cdot \vec{\pi}$, there are

$$\begin{aligned} \varepsilon_0(0) &= \beta, \varepsilon_1(0) = \beta S + V - \vec{\Omega} \cdot \vec{J}, \varepsilon_i(0) = 0, i \geq 2, \\ o_1(0) &= \vec{\alpha} \cdot \vec{\pi}, o_i(0) = 0, i \geq 2. \end{aligned} \quad (9)$$

With the initial conditions, we have obtained the diagonal Hamiltonian:

$$\varepsilon(\infty) = M\varepsilon_0(\infty) + \varepsilon_1(\infty) + \frac{1}{M}\varepsilon_2(\infty) + \frac{1}{M^2}\varepsilon_3(\infty) + \dots \quad (11)$$

The diagonal part describing the positive energy states H can be written as

$$H = H_{\text{NR}} + H_{\text{Dy}} + H_{\text{SO}} + H_{\text{Dw}} + H_{\text{R}} + H_{\text{Z}} + H_{\text{SR}}, \quad (12)$$

where

$$\begin{aligned} H_{\text{NR}} &= \frac{1}{2M} \vec{\pi}^2 + S + V, \\ H_{\text{Dy}} &= -\frac{S}{2M^2} \vec{\pi}^2 + \frac{i\hbar}{2M^2} \nabla S \cdot \vec{\pi}, \\ H_{\text{SO}} &= +\frac{\hbar}{8M^2} \vec{\sigma} \cdot \left[\vec{\pi} \times \left(\vec{E}_S + \vec{E}_V \right) - \left(\vec{E}_S + \vec{E}_V \right) \times \vec{\pi} \right], \\ H_{\text{Dw}} &= \frac{\hbar^2}{8M^2} \nabla \cdot \left(\vec{E}_S - \vec{E}_V + \vec{E}_\Omega \right), \\ H_{\text{R}} &= -\vec{\Omega} \cdot \vec{j}, \\ H_{\text{Z}} &= -\frac{\hbar}{2M^2} (M - S) \vec{\sigma} \cdot \vec{B}, \\ H_{\text{SR}} &= -\frac{\hbar}{8M^2} \vec{\sigma} \cdot \left(\vec{\pi} \times \vec{E}_\Omega - \vec{E}_\Omega \times \vec{\pi} \right). \end{aligned} \quad (13)$$

Here $\vec{E}_S = \nabla S$, $\vec{E}_V = -\nabla V$, and $\vec{E}_\Omega = \left(\vec{\Omega} \times \vec{r} \right) \times \vec{B}$ with the assumption $\vec{B} = \nabla \times \vec{V}$. The angular momentum $\vec{j} = \left(\vec{r} \times \vec{\pi} + \vec{s} \right)$. H_{NR} corresponds to the non-relativistic approximation. H_{Dy} is the dynamical term. H_{SO} represents the spin-orbital coupling. H_{Dw} is the Darwin term. H_{R} is the rotational term. The Zeeman effect is related to the operator H_{Z} . H_{SR} is claimed as the spin-rotation coupling. For the system without rotation, H_{R} and H_{SR} disappear. From the decomposition of Hamiltonian, we can explore the important physics hidden in the cranking Dirac Hamiltonian.

III. NOVEL PHENOMENA IN ROTATING NUCLEI

Based on the diagonal cranking Dirac Hamiltonian given in Eq. (12), we explore the novel phenomena in

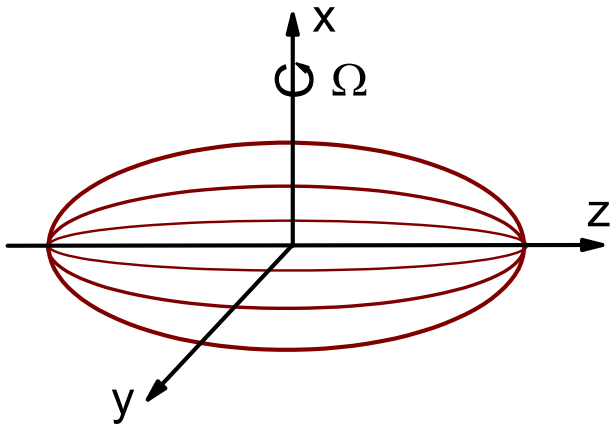


FIG. 1: (Color online) An axially deformed nucleus rotating around x -axis. z is its symmetric axis. Ω is the rotational angular velocity.

rotating nuclei. In Refs. [35, 36], we have probed the physical meanings of these terms H_{NR} , H_{Dy} , H_{SO} , and H_{Dw} , and disclosed their influences on the spin and pseudospin symmetries [37–40]. However, since the rotation and the spatial component of the vector field $\vec{V}(\vec{r})$ are not taken into account in these references, these terms H_{R} , H_{Z} , and H_{SR} do not appear there, while they have received great attention in atomic and molecular and condensed matter physics. Hence, it is necessary to explore the physical effects of these additional terms and their contributions to the single-particle spectra in atomic nuclei. For simplicity without losing generality, the nucleus is assumed to be symmetrical around z axis, the rotation is around x -axis, a prolate or oblate deformation occurs in z -axis direction, as shown in Fig. 1. The nucleus rotates around x -axis with the rotational angular velocity Ω , i.e., $\vec{\Omega} = \Omega_x \vec{e}_x$. For the magnetic field-like \vec{B} , only the x -direction $\vec{B} = B_x \vec{e}_x$ is considered. With the assumption, the Hamiltonian becomes

$$\begin{aligned}
 H = & \frac{\vec{\pi}^2}{2M} + \Sigma(r) - \Omega_x j_x \\
 & - \frac{S}{2M^2} \vec{\pi}^2 + \frac{i}{2M^2} \nabla S \cdot \vec{\pi} + \frac{1}{8M^2} \nabla^2 \Sigma \\
 & + \frac{1}{4M^2} \vec{\sigma} \cdot (\nabla \Delta \times \vec{\pi}) - \frac{1}{2M^2} (M - S) \sigma_x B_x \\
 & + \frac{B_x \Omega_x}{4M^2} + \frac{B_x \Omega_x}{4M^2} \vec{\sigma} \cdot (\vec{r}_{yz} \times \vec{\pi}). \quad (14)
 \end{aligned}$$

To simplify the computation and avoid affecting the conclusion, we have replaced $\vec{\pi}$ with \vec{p} . The energy spectra of the Hamiltonian in Eq. (14) are obtained through basis expansions. It is important to note that for axisymmetrically deformed nuclei, the third component of angular momentum is no longer a good quantum number due to rotation. Here, only axisymmetric quadrupole deformation is considered, parity remains a good quantum number. ^{64}Ge is chosen as an illustrated example. The

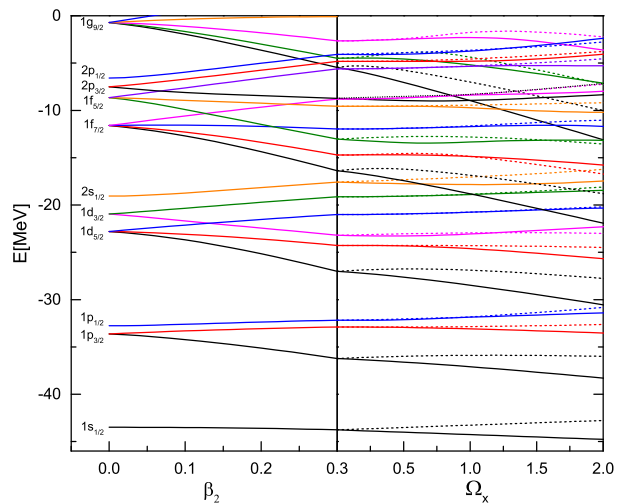


FIG. 2: (Color online) The single-particle spectra and their evolutions to the quadrupole deformation β_2 and the rotational angular velocity around x -axis Ω_x .

corresponding potentials are adopted as

$$\begin{aligned}
 S(\vec{r}) &= S_0(r) + S_2(r) P_2(\theta), \\
 V(\vec{r}) &= V_0(r) + V_2(r) P_2(\theta), \quad (15)
 \end{aligned}$$

where $P_2(\theta) = \frac{1}{2}(3\cos^2\theta - 1)$. The radial parts in Eq. (15) take a Woods-Saxon form,

$$\begin{aligned}
 S_0(r) &= S_{\text{WS}} f(r), \quad S_2(r) = -\beta_2 S_{\text{WS}} k(r), \\
 V_0(r) &= V_{\text{WS}} f(r), \quad V_2(r) = -\beta_2 V_{\text{WS}} k(r), \quad (16)
 \end{aligned}$$

with $f(r) = \frac{1}{1 + \exp(\frac{r-R}{a})}$, and $k(r) = r \frac{df(r)}{dr}$. Here V_{WS} and S_{WS} are, respectively, the typical depths of the scalar and vector potentials in the relativistic mean field chosen as 350 and -405 MeV, the diffuseness of the potential a is fixed as 0.67 fm, and β_2 is the axial deformation parameter of the potential. The radius $R \equiv r_0 A^{1/3}$ with $r_0 = 1.27$ fm. With these parameters are determined, the energy spectra of Hamiltonian H can be calculated.

The single-particle spectra and their evolutions with the quadrupole deformation β_2 and the rotational angular velocity around the x -axis Ω_x are presented in Fig. 2. The left panel shows the Nilsson levels with deformation β_2 ranging from 0 to 0.3. The right panel illustrates the variation of single-particle spectra with Ω_x for $\beta_2 = 0.3$. From the spherical to axial deformation, the levels experience splitting, as the well-known Nilsson levels are clearly visible. For axially deformed nuclei, there are signature splittings in doubly degenerate Nilsson levels. Compared to unaligned spin states, the signature splitting is larger for spin aligned states. In particular, for the spin aligned state with the least third component of total angular momentum, the signature splitting is the largest and most sensitive to Ω_x as shown in Fig. 2 for the single particle level $1g_{9/2,1/2}$. The single-particle energy drops faster with increasing Ω_x due to the stronger influence of

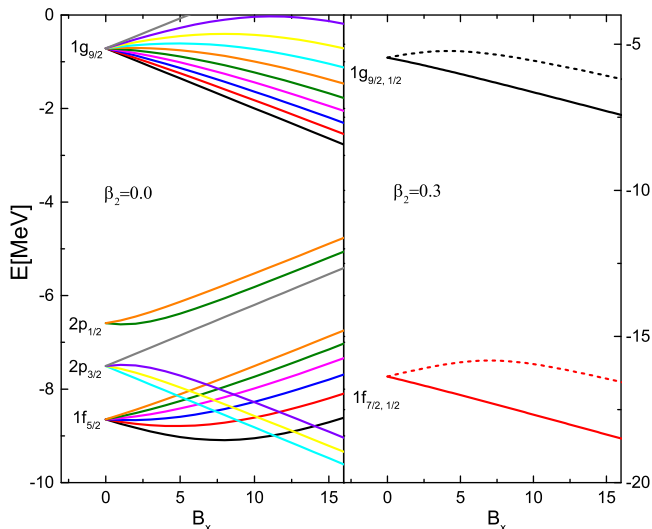


FIG. 3: (Color online) The single-particle spectra and their evolutions to the magnetic field-like B_x for the spherical nuclei and deformed nuclei with $\beta_2 = 0.3$.

the Coriolis force on the energy spectrum, which is consistent with the prediction of the cranking shell model. Signature splitting is an important phenomenon in rotating nuclei. Our present calculations based on the diagonal Dirac Hamiltonian in Eq. (14) can reproduce the signature splitting, which represents the first time that signature splitting in nuclei has been understood in a relativistic framework.

In addition to the signature splitting caused by this cranking item H_R , the additional H_Z deserves special attention. It is the cause of the Zeeman effect in the atomic and molecular physics. To understand the role of H_Z in atomic nuclei, the single-particle spectra and their evolutions to the magnetic field-like B_x for the spherical nuclei and deformed nuclei with $\beta_2 = 0.3$ are presented in Fig. 3. In the left panel, the result for spherical nuclei is shown, while in the right panel, the results for deformed nuclei with $\beta_2 = 0.3$ are shown. When $B_x \neq 0$, every degenerate spherical level with the total angular momentum j is split into $2j + 1$ levels. As B_x increases, the level split increases as well. For deformed nuclei, the doubly degenerate Nilsson levels split when $B_x \neq 0$. The some split are remarkable, while others are considerably small or even unobservable. However, for the spin aligned state with the least third component of total angular momentum, the level split is significant and sensitive to B_x , as seen in the right panel in Fig. 3 for $1f_{7/2, 1/2}$ and $1g_{9/2, 1/2}$. For the convenience of describing the problem, the splitting caused by the H_Z is claimed as Zeeman splitting-like. When B_x is large enough, the Zeeman splitting-like becomes considerable and may lead to an observable Zeeman effect-like. The observation of Zeeman effect-like can help us to understand the level structure and the strength of the magnetic field-like B_x . It is well worth experimentally probing the Zeeman effect-like in the nu-

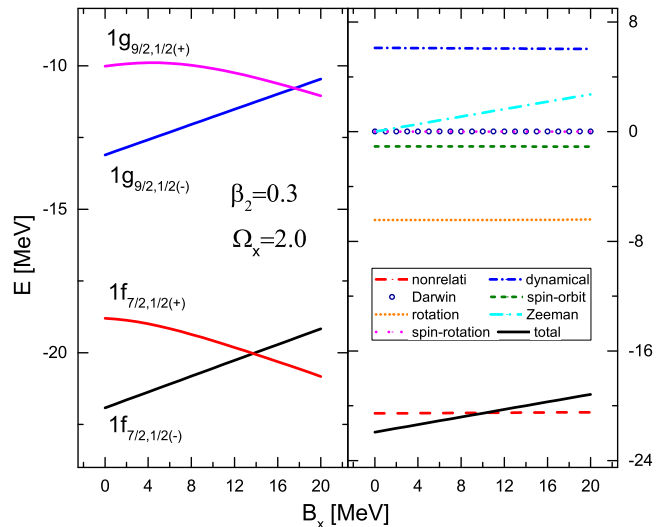


FIG. 4: (Color online) The energies of single particle levels and their components evolve to the magnetic field-like B_x for the rotational nuclei with $\beta_2 = 0.3$ and $\Omega_x = 2.0$ MeV. The left panel shows the signature doublets $1f_{7/2, 1/2}$ and $1g_{9/2, 1/2}$. The right panel illustrates the contributions of every component to the single-particle level $1f_{7/2, 1/2(-)}$.

clei.

Moreover, we have investigated the influence of the magnetic field-like B_x on signature splitting in rotating nuclei with $\beta_2 = 0.3$ and $\Omega_x = 2.0$ MeV. The left panel of Fig. 4 displays the level splittings for the signature doublets $1f_{7/2, 1/2}$ and $1g_{9/2, 1/2}$ and their evolutions to B_x . As B_x increases, the levels for the $1f_{7/2, 1/2(-)}$ and $1g_{9/2, 1/2(-)}$ go up, while those for the $1f_{7/2, 1/2(+)}$ and $1g_{9/2, 1/2(+)}$ go down. There are also the levels of the signature doublet crosses at a specific B_x . To clarify the evolution of level splittings to B_x , the contributions of every component to the single-particle level $1f_{7/2, 1/2(-)}$ are displayed in the right panel of Fig. 4. The non-relativistic, dynamical, and rotational terms have significant contributions to the total energy. The spin-orbit coupling and the term relating to Zeeman effect-like contribute relatively little to the total energy. The Darwin term and the spin-rotation coupling contribute very little to the total energy. Except for the term relating to Zeeman effect-like, the other contributions to the total energy are independent of B_x . The energy increasing with B_x comes entirely from the contribution of the term relating to Zeeman effect-like, which is the cause of Zeeman effect-like in rotating nuclei.

To better understand the Zeeman effect-like in rotating nuclei, the left panel of Fig. 5 displays the signature splittings contributed by the term relating to Zeeman effect-like for the two signature doublets $1f_{7/2, 1/2}$ and $1g_{9/2, 1/2}$ with $\beta_2 = 0.3$ and $\Omega_x = 2.0$ MeV. With the increase of B_x , the energy increases for the $1f_{7/2, 1/2(-)}$ and $1g_{9/2, 1/2(-)}$, while the energy decreases for the $1f_{7/2, 1/2(+)}$ and $1g_{9/2, 1/2(+)}$. When $B_x = 20$

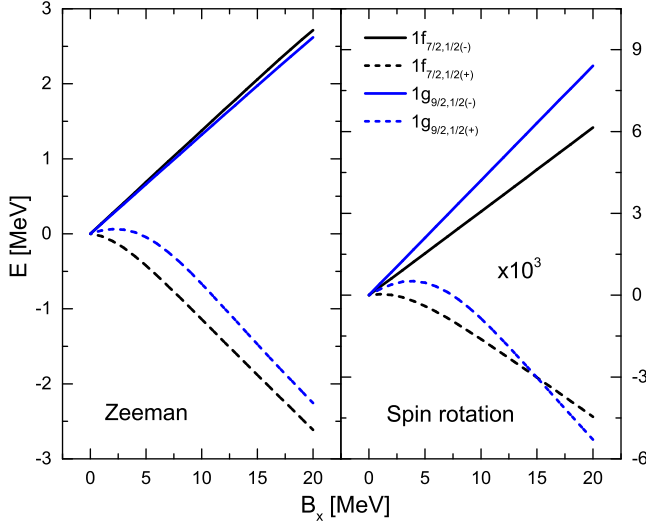


FIG. 5: (Color online) The energies contributed by the operator relating to Zeeman effect-like and the spin-rotation coupling, and their evolutions with the magnetic field-like B_x in the single particle levels $1f_{7/2,1/2(-)}$, $1f_{7/2,1/2(+)}$, $1g_{9/2,1/2(-)}$, and $1g_{9/2,1/2(+)}$. The other physical quantities are the same as Fig. 4.

MeV, the increasing or reducing energy is about 3.0 MeV, which is quite observable. These indicate that the Zeeman effect-like plays a significant role in the signature splitting in rotating nuclei. For comparison, the spin-rotation coupling effect is displayed in the right panel in Fig. 5. The trend with B_x is similar, but the magnitudes are much smaller than 3 orders of magnitude.

IV. SPIN CURRENT

Although the spin-rotation coupling contributes less to the signature splitting, it may cause the occurrence of spin current. To investigate the spin current, we extract the operator of spin-rotation coupling from the total Hamiltonian as follows:

$$H_{SR} = -\frac{\hbar}{8M^2} \vec{\sigma} \cdot (\vec{\pi} \times \vec{E}_\Omega - \vec{E}_\Omega \times \vec{\pi}). \quad (17)$$

By the definition, the speed relating to the spin-rotation coupling is

$$\begin{aligned} \vec{v}_s &= \frac{1}{i\hbar} [\vec{r}, H_{SR}] \\ &= \frac{1}{i\hbar} \left[\vec{r}, \frac{\hbar}{8M^2} \vec{\sigma} \cdot (i\hbar \nabla \times \vec{E}_\Omega + 2\vec{E}_\Omega \times \vec{\pi}) \right] \\ &= \frac{1}{4iM^2} \left[\vec{r}, \vec{\sigma} \cdot (\vec{E}_\Omega \times \vec{p}) \right]. \end{aligned} \quad (18)$$

If the only $\vec{\Omega} = \Omega_x \vec{e}_x$ is considered, there is

$$\vec{E}_\Omega = \Omega_x [-(B_y y + B_z z) \vec{e}_x + B_x y \vec{e}_y + B_x z \vec{e}_z]. \quad (19)$$

The speed relating to the spin-rotation coupling is

$$\begin{aligned} \vec{v}_s &= \frac{\hbar \Omega_x}{4M^2} \left[(\sigma_y z - \sigma_z y) B_x \vec{e}_x \right. \\ &\quad - (\sigma_z B_y y + \sigma_z B_z z + \sigma_x B_x z) \vec{e}_y \\ &\quad \left. + (\sigma_x B_x y + \sigma_y B_y y + \sigma_y B_z z) \vec{e}_z \right] \end{aligned} \quad (20)$$

Due to rotation in the x -direction, only $\vec{B} = B_x \vec{e}_x$ is dominant.

$$\vec{v}_s = \frac{\hbar \Omega_x B_x}{4M^2} [(\sigma_y z - \sigma_z y) \vec{e}_x + \sigma_x (y \vec{e}_z - z \vec{e}_y)] \quad (21)$$

$$v_{x//}^s = \frac{B_x \Omega_x}{4M^2} (\sigma_y z - \sigma_z y) \vec{e}_x, \quad (22)$$

$$v_{x\perp}^s = \frac{B_x \Omega_x}{4M^2} \sigma_x (y \vec{e}_z - z \vec{e}_y) = \frac{B_x \Omega_x}{4M^2} \sigma_x r_{yz} \vec{e}_\phi^{yz}. \quad (23)$$

The spin current is defined as

$$J_s = M_{r_{yz}} Tr \sigma_x v_{x\perp}^s = M_{r_{yz}} \frac{B_x \Omega_x}{2M^2} r_{yz} \vec{e}_\phi^{yz}, \quad (24)$$

$$|J_s| = M_{r_{yz}} \frac{B_x \Omega_x}{2M^2} r_{yz}. \quad (25)$$

For a single nucleon populating at r_{yz} , an estimate of the size of the spin current

$$|J_s| = \frac{B_x \Omega_x}{2M} r_{yz}. \quad (26)$$

Assuming $\Omega_x = 2$ MeV, $B_x = 20$ MeV, and $r_{yz} = 5$ fm, the calculated spin current $|J_s| \approx 5.41 \times 10^{-4}$ MeV = 0.541 keV. With the advancement of laser control technology, we can prepare strong enough lasers to control nuclear reactions and nuclear structures. It may be possible to regulate nucleon spin and spin current in the near future.

V. SUMMARY

In summary, we have combined the cranking covariant density functional theory with similar renormalization group to decompose the Dirac Hamiltonian from the cranking CDFT into several Hermit components, including the non-relativistic term, the dynamical term, the spin-orbit coupling, and the Darwin term. Especially, we have obtained the rotational term, the term relating to Zeeman effect-like, and the spin-rotation coupling due to the consideration of rotation and spatial component of vector potential. Based on these operators, we have explored the novel phenomena that may occur in rotating nuclei.

One of the most fascinating phenomena is signature splitting. It is shown that the signature splitting is larger for spin aligned states than that for unaligned spin states. Especially, the spin aligned state with the least third

component and the largest total angular momentum experiences the largest signature splitting. The energy of this state decreases faster with the increase of Ω_x , which is attributed to the increased strength of the Coriolis force.

In addition to the signature splitting, we also investigated the level splitting caused by the operator relating to Zeeman effect-like. For spherical nuclei, the degenerate level is split into $2j + 1$ levels, and the level splitting increases with the increase of magnetic field-like B_x . For deformed nuclei, the doubly degenerate levels split. For the spin aligned state with the least third component, the level splitting is remarkable and sensitive to B_x . When B_x is sufficiently large, the Zeeman splitting-like becomes significant enough to produce an observable Zeeman effect-like for both spherical and deformed nuclei. The observation of the Zeeman effect-like can provide valuable insights in the level structure and the strength of the magnetic field-like B_x in rotating nuclei.

Moreover, we have investigated the influence of the magnetic field-like B_x on signature splitting in rotating nuclei with $\beta_2 = 0.3$ and $\Omega_x = 2.0$ MeV. We observed that the levels with the signature (-) go up while those with the signature (+) go down with the increase of B_x . The trend of the level energies with B_x is fully attributed to the contribution of the term related to Zeeman effect. Although these terms, such as the non-relativistic, the dynamical, the rotational, and the spin-orbit coupling, contribute considerably to the signature splittings, they are almost independent of B_x . Furthermore, we have ex-

tracted the signature splitting contributed by the term relating to Zeeman effect. With the increase of B_x , the energy increase for the state with signature (-) and the energy decrease for the state with signature (+) are considerably observable. These imply the operator relating to Zeeman effect play an important role at signature splitting in rotating nuclei.

Based on the spin-rotation coupling, we calculate the spin current, evaluate the magnitude of spin current, and point out the possibility of regulating the nuclear spin and spin current in the near future with advances in laser control technology.

The theoretical predictions on these novel phenomena have significant reference value for experimental detection of such phenomena in atomic nuclei.

VI. ACKNOWLEDGMENTS

This work was partly supported by the National Natural Science Foundation of China under Grants No. 11935001 and No.11575002, Anhui project (Z010118169), Heavy Ion Research Facility in Lanzhou (HIRFL) (HIR2021PY007), the project of Key Laboratory of High Precision Nuclear Spectroscopy in Chinese Academy of Sciences, and the Graduate Research Foundation of Education Ministry of Anhui Province under Grant No. YJS20210096.

-
- [1] I. Tanihata, H. Savajols, R. Kanungo, *Prog. Part. Nucl. Phys.* **68**, 215 (2013).
- [2] T. Nakamura, H. Sakurai, H. Watanabe, *Prog. Part. Nucl. Phys.* **97**, 53 (2017).
- [3] G. L. Wilson, W. N. Catford, N. A. Orr, and *et al.*, *Phys. Lett. B* **759**, 417 (2016).
- [4] B. Longfellow, D. Weisshaar, A. Gade, B. A. Brown, D. Bazin, K. W. Brown, B. Elman, J. Pereira, D. Rhodes, M. Spieker, *Phys. Rev. Lett.* **125**, 232501 (2020).
- [5] A. Ozawa, T. Kobayashi, T. Suzuki, K. Yoshida, and I. Tanihata, *Phys. Rev. Lett.* **84**, 5493 (2000).
- [6] R. F. Garcia Ruiz, M. L. Bissell, K. Blaum, A. Ekström, N. Frömmgen, G. Hagen, M. Hammen, K. Hebel, J.D. Holt, G.R. Jansen, M. Kowalska, K. Kreim, W. Nazarewicz, R. Neugart, G. Neyens, W. Nörtershäuser, T. Papenbrock, J. Papuga, A. Schwenk, J. Simonis, K.A. Wendt, and D.T. Yordanov, *Nature Physics* **12**, 594 (2016).
- [7] E. Leistenschneider, E. Dunling, G. Bollen, B. A. Brown, J. Dilling, A. Hamaker, J. D. Holt, A. Jacobs, A. A. Kwiatkowski, T. Miyagi, W. S. Porter, D. Puentes, M. Redshaw, M. P. Reiter, R. Ringle, R. Sandler, C. S. Sumithrarachchi, A. A. Valverde, and I. T. Yandow, *Phys. Rev. Lett.* **126**, 042501 (2021).
- [8] E. Olsen, M. Pfützner, N. Birge, M. Brown, W. Nazarewicz, and A. Perhac, *Phys. Rev. Lett.* **110**, 222501 (2013); Erratum, E. Olsen, M. Pfützner, N. Birge, M. Brown, W. Nazarewicz, and A. Perhac, *Phys. Rev. Lett.* **111**, 139903 (2013).
- [9] Y. G. Ma, D. Q. Fang, X. Y. Sun, *et al.*, *Phys. Lett. B* **743**, 306 (2015).
- [10] P. J. Twin, B.M. Nyakó, A. H. Nelson, J. Simpson, M. A. Bentley, H. W. Cranmer-Gordon, P. D. Forsyth, D. Howe, A. R. Mokhtar, J. D. Morrison *et al.*, *Phys. Rev. Lett.* **57**, 811 (1986).
- [11] B. Singh, R. Zywina, and R. B. Firestone, Table of Superdeformed Nuclear Bands and Fission Isomers: Third Edition (October 2002), *Nucl. Data Sheets* **97**, 241 (2002).
- [12] A. Johnson, H. Ryde, and J. Sztarkier, *Phys. Lett. B* **34**, 605 (1971).
- [13] I. Y. Lee, M. M. Aleonard, M. A. Deleplanque, Y. El-Masri, J. O. Newton, R. S. Simon, R. M. Diamond, and F. S. Stephens, *Phys. Rev. Lett.* **38**, 1454 (1977).
- [14] T. Bengtsson and I. Ragnarsson, *Phys. Scr.* **T5**, 165 (1983).
- [15] A. Afanasjev, D. Fossan, G. Lane, and I. Ragnarsson, *Phys. Rep.* **322**, 1 (1999).
- [16] R. Bengtsson, H. Frisk, F. R. May, and J. A. Pinston, *Nucl. Phys. A* **415**, 189 (1984).
- [17] S. Frauendorf, J. Meng, and J. Reif, in Proceedings of the Conference on Physics From Large γ -Ray Detector

- Arrays, edited by M. A. Deleplanque, Report LBL35687 (University of California, Berkeley, 1994), Vol. II, p. 52.
- [18] S. Frauendorf, *Rev. Mod. Phys.* **73**, 463 (2001).
- [19] S. Frauendorf and J. Meng, *Nucl. Phys. A* **617**, 131 (1997).
- [20] G. Andersson, S. E. Larsson, G. Leander, P. Möller, S. G. Nilsson, I. Ragnarsson, S. Åberg, R. Bengtsson, J. Dudek, B. Nerlo-Pomorska, K. Pomorski, and Z. Szymanski, *Nucl. Phys. A* **268**, 205 (1976).
- [21] R. Bengtsson and S. Frauendorf, *Nucl. Phys. A* **327**, 139 (1979).
- [22] H. Hara and Y. Sun, *Int. J. Mod. Phys. E* **04**, 637 (1995).
- [23] E. Caurier, J. Menéndez, F. Nowacki, and A. Poves, *Phys. Rev. C* **75**, 054317 (2007).
- [24] A. V. Afanasjev, J. König, P. Ring, L. M. Robledo, and J. L. Egido, *Phys. Rev. C* **62**, 054306 (2000).
- [25] S. Sakai, K. Yoshida, and M. Matsuo, *Prog. Theor. Exp. Phys.* **2020**, 063D02 (2020).
- [26] E. Ideguchi, D. G. Sarantites, W. Reviol, A. V. Afanasjev, M. Devlin, C. Baktash, R. V. F. Janssens, D. Rudolph, A. Axelsson, M. P. Carpenter et al., *Phys. Rev. Lett.* **87**, 222501 (2001).
- [27] D. Ray and A. V. Afanasjev, *Phys. Rev. C* **94**, 014310 (2016).
- [28] K. Starosta, T. Koike, C. J. Chiara, D. B. Fossan, D. R. LaFosse, A. A. Hecht, et al., *Phys. Rev. Lett.* **86**, 971 (2001).
- [29] J. Meng, J. Peng, S. Q. Zhang, and S.-G. Zhou, *Phys. Rev. C* **73**, 037303 (2006).
- [30] A. D. Ayangeakaa, U. Garg, M. D. Anthony, S. Frauendorf, J. T. Matta, B. K. Nayak, D. Patel, Q. B. Chen, S. Q. Zhang, P. W. Zhao et al., *Phys. Rev. Lett.* **110**, 172504 (2013).
- [31] I. Kuti, Q. B. Chen, J. Timár, D. Sohler, S. Q. Zhang, Z. H. Zhang, P. W. Zhao, J. Meng, K. Starosta, T. Koike et al., *Phys. Rev. Lett.* **113**, 032501 (2014).
- [32] C. Liu, S. Y. Wang, R. A. Bark, S. Q. Zhang, J. Meng, B. Qi, P. Jones, S. M. Wyngaardt, J. Zhao, C. Xu et al., *Phys. Rev. Lett.* **116**, 112501 (2016).
- [33] P. W. Zhao, Z. P. Li, J. M. Yao, and J. Meng, *Phys. Rev. C* **82**, 054319 (2010).
- [34] J. Meng and P. Zhao, *Phys. Scr.* **91**, 053008 (2016)
- [35] J. Y. Guo, *Phys. Rev. C* **85**, 021302(R) (2012).
- [36] J. Y. Guo, S. W. Chen, Z. M. Niu, D. P. Li, Q. Liu, *Phys. Rev. Lett.* **112**, 062502 (2014).
- [37] S. W. Chen and J. Y. Guo, *Phys. Rev. C* **85**, 054312 (2012).
- [38] D. P. Li, S. W. Chen, and J. Y. Guo, *Phys. Rev. C* **87**, 044311 (2013) .
- [39] Bo Huang, Jian-You Guo, and Shou-Wan Chen, *Phys. Rev. C* **105**, 054313 (2022).
- [40] D. P. Li, S. W. Chen, Z. M. Niu, Q. Liu, J. Y. Guo, *Phys. Rev. C* **91**, 024311 (2015) .
- [41] Yixin Guo and Haozhao Liang, *Phys. Rev. C* **99**, 054324 (2019).
- [42] Z. X. Ren and P. W. Zhao, *Phys. Rev. C* **102**, 021301(R) (2020).
- [43] I. Ztic and H. Dery, *Nat. Mater.* **10**, 647 (2011).
- [44] W. Han, S. Maekawa, and X.-C. Xie, *Nat. Mater.* **19**, 1 (2019).
- [45] J. Sinova, S. O. Valenzuela, J. Wunderlich, C. H. Back, and T. Jungwirth, *Rev. Mod. Phys.* **87**, 1213 (2015).